Topological Generators and Cut-Graphs of Arbitrary Triangle Meshes

Giuseppe Patanè Michela Spagnuolo Bianca Falcidieno
IMATI-CNR, Genova - Italy
{*patane,spagnuolo,falcidieno*}*@ge.imati.cnr.it*

Abstract

Recent advances in the parameterization and adaptive sampling of disc-like surfaces have brought a renewed interest on the global parameterization problem and, more specifically, on the cut-graph search. This paper focuses on the calculation of a family of generators and cut-graphs for the global parameterization of arbitrary triangle meshes. This result is achieved by combining the construction of harmonic scalar fields $f : \mathcal{M} \to \mathbb{R}$ of known maxima and minima with the quasi Morse-Smale complex of $(\mathcal{M}, f)$.

The proposed technique has a simple implementation and outperforms previous work in terms of smoothness of the cut-graphs, stability with respect to the surface sampling, tessellation, topological noise (e.g., tiny handles), and capability of handling boundary components. Since we generate a family of cut-graphs, we also provide a comparison between the parameterizations of $\mathcal{M}$ induced by two cut-graphs.

1 Introduction

Triangulated surfaces are generated by polygonizing implicit functions, sampling parametric surfaces, or scanning real 3D objects with optical devices. All these generation processes provide complex discrete models with arbitrary genus and curvature that are usually unsatisfactory for shape modeling and analysis. In fact, they may have a redundant number of vertices together with an irregular vertex sampling and mesh connectivity. Therefore, a basic task consists of improving an arbitrary triangulated surface $\mathcal{M}$ in terms of sampling density and distribution, regular or semi-regular connectivity, and mesh quality. These problems can be addressed by decomposing the surface into a family of disc-like patches (i.e., *local parameterization*), or by defining a cut on the manifold which is successively unfolded onto a planar domain (i.e., *global parameterization*).

Given a triangular mesh $\mathcal{M} := \{M, T\}$, where $M := \{\mathbf{p}_i,\, i = 1, \ldots, n\}$ is a set of n vertices and T is an *abstract simplicial complex*, the *global parameterization* problem defines a simplicial isomorphism $\varphi : \mathcal{M} \to \mathcal{P} \subseteq \mathbb{R}^2$, with $\mathcal{P}$ parameterization domain; that is, an injective map

$$\begin{aligned} \varphi|_M : \quad & M \to \Omega \subseteq \mathbb{R}^2 \\ & \mathbf{p}_i \mapsto \mathbf{t}_i \end{aligned}$$

with $\Omega := \{\mathbf{t}_i,\, i = 1, \ldots, n\}$ and such that $\mathcal{P} := (\Omega, T)$ is a planar disc homeomorphic to $\mathcal{M}$. The map φ is extended from the vertices M to the surface $\mathcal{M}$ by using barycentric coordinates. If $\mathcal{M}$ has genus $g \geq 1$, or at least two boundary components, we need to cut $\mathcal{M}$ along a path γ for unfolding it onto a disc. The curve γ, which converts $\mathcal{M}$ to a disc-like surface $\overline{\mathcal{M}} := \mathcal{M} \setminus \gamma$, is called the *cut-graph* of $\mathcal{M}$. Among the possible cut-graphs, those that include the *generators* of each topological handle $\mathcal{H}$ of $\mathcal{M}$ are particularly interesting; these generators are the *meridian* and *longitude* cuts which are around and along $\mathcal{H}$, respectively. Once a cut-graph γ has been found, $\overline{\mathcal{M}}$ is embedded onto $\mathcal{P}$ by any parameterization technique of disc-like surfaces. These methods differ on the way they minimize the induced parametric distortion, usually located by high-curvature regions of $\mathcal{M}$; for a detailed review, we refer the reader to [8].

Recent advances on the parameterization of disc-like surfaces [8, 23, 26], which efficiently reduces the distortion of the embedding, and adaptive sampling [1], which distributes the new vertices on the parameterization domain depending on the local stretch, have brought a renewed interest on the global parameterization problem and, more specifically, on the cut-graph search. Therefore, in this paper we focus on the search of a family of generators and cut-graphs for the global parameterization of arbitrary triangle meshes.

Among the wide uses of the global parameterization, it is worth to mention *surface remeshing*, *texture mapping*, and *compression*. For surface remeshing [1], the parameter domain $\mathcal{P}$ is resampled and the new triangulation is projected back into 3D space by φ^{-1}. If $\mathcal{M}$ is parameterized into a 2D square by using a stretch-minimization method, the embedding can be used for texture mapping [12, 22] and $\mathcal{M}$ can be represented as a *geometry image* [21], which stores the geometry and any other vertex attribute (e.g., normal

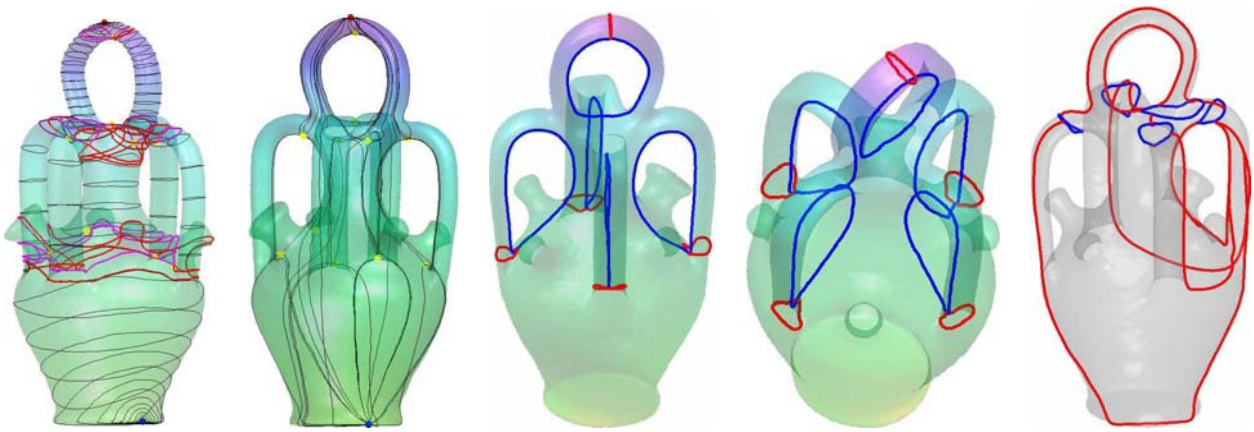

(a) (b) (c) (d) (e)

Figure 1. (a) Iso-contours, critical points, and loops at the saddle points of a harmonic scalar field on a 5-genus surface. (b) Quasi Morse-Smale complex and (c-d) generators of the topological handles. Meridians (resp., longitudes) are depicted in red (resp., blue). (e) Cut-graph which minimizes the parameterization distortion.

vectors, colors) as RGB values of a grid structure. Even thought these applications can be also approached by the local parameterization, we note that working with a unique embedding avoids to segment the input shape, which requires a non-trivial alignment of surface patches with shape features [18, 21], does not require to control the smoothness of the embedding among adjacent patches [14, 21], and achieves high compression rates [10].

Related work. Arbitrary cut-graphs are evaluated in $O(gn)$ time, paths interpolating a common base point can be optimized in polynomial time [3], and the search of the cut of minimal length is NP-hard [6]. In [24], the cut-graph is a tree defined by the iso-contours of the geodesic distance from a source point and connected by using a geodesic-based procedure. In [10], γ is built by an iterative procedure that removes at each step a triangle, while maintaining the set of removed faces homeomorphic to a disc. In [17], the cut-graph interpolates the critical points of a harmonic scalar field whose maxima and minima are selected by the user among the vertices of $\mathcal{M}$ (see Section 2). Previous work is mainly limited to deal with closed surfaces and the final cut-graph is usually affected by the connectivity of the input surface. To overcome these limitations, [19] builds γ on the iso-contours of a scalar field $f : \mathcal{M} \rightarrow \mathbb{R}$, that cut the topological handles of $\mathcal{M}$ along meridian loops, and on the completion of the cut-graph on the planar domain. The method defines a family of smooth cut-graphs and applies to arbitrary surfaces with boundary components.

In [13], an algebraic algorithm extracts and classifies the generators of the input surface $\mathcal{M}$ using a volumetric representation. The shortest set of loops of the fundamental group of a closed and analytic Riemannian 2-manifold can be evaluated in $O(n \log n)$ time [7] by using the Dijkstra's shortest path algorithm. In [25], the cut-graph of a closed surface $\mathcal{M}$ is built as the minimum spanning tree of the $2g$ boundaries generated by duplicating the g longitudes found by the EdgeBreaker algorithm [15]. This method also provides the generators of $\mathcal{M}$ without classifying them as meridians and longitudes. The classification is done by calculating the *link-number* of two loops; to this end, the set of loops are mapped onto a projection plane avoiding degenerate cases (e.g., line segments of a loop projected to a point) and overlaps among projected line segments. Therefore, an extensive search finds a valid projection plane. Finally, under certain sampling conditions, [9] finds the generators of a point cloud representing a 2-manifold without boundary.

Overview and contribution. The aim of this paper is threefold. The first aim is to define a simple method to build a family of smooth cut-graphs of a triangle mesh $\mathcal{M}$ by cutting the topological handles along the meridian loops of the saddle points of a scalar field $f : \mathcal{M} \rightarrow \mathbb{R}$ (see Section 2 and 3). The second result is the extraction of the generators of the topological handles of $\mathcal{M}$ by combining the construction of harmonic scalar fields of known maxima and minima with the quasi Morse-Smale complex $\mathcal{C}$ of $(\mathcal{M}, f)$. These generators are then converted into a cut-graph of $\mathcal{M}$ by applying the method described in Section 3, or using the minimum spanning tree of a weighted and undirected graph induced by $\mathcal{C}$ (see Section 4). Since the proposed techniques generate a family of cut-graphs, the third result is a compar-

ison of the parameterization of $\mathcal{M}$ induced by two different cut-graphs γ, β, and based on the analysis of the Laplacian matrices of $\mathcal{M} \setminus \gamma$ and $\mathcal{M} \setminus \beta$ (see Section 5).

As discussed in Section 6 and throughout the paper, our main contribution with respect to previous work is a computationally efficient construction of a family of smooth cut-graphs and topological generators of arbitrary triangulated surfaces, without assumptions on the vertex sampling, tessellation, and presence of boundary components. Furthermore, the proposed approach is stable with respect to geometric and topological noise (e.g., tiny handles), and the computational cost varies from $O(n)$ to $O(n \log n)$, depending on the sparsity percentage of the Laplacian matrix associated to $\mathcal{M}$. An example of the generators and cut-graph search is given in Figure 1.

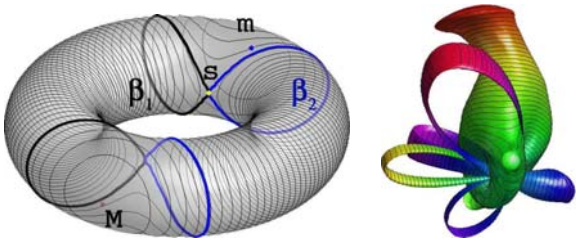

(a) (b)

Figure 2. (a) Iso-contours close to a minimum m (resp., maximum M, saddle s). The iso-contour related to the saddle s is split into two meridian loops β_1, β_2. (b) Sixth spherical harmonic of the surface shown in Figure 1.

2 Theoretical background

This section introduces the theoretical background used to find a family of topological generators and cut-graphs of arbitrary triangle meshes.

Defining smooth scalar fields on $\mathcal{M}$. In [17], a harmonic scalar field f is calculated by solving the equation $\Delta f = 0$, where Δ is the Laplace-Beltrami operator, subject to the Dirichlet boundary conditions $\mathcal{B} := \{f(\mathbf{p}_i) = a_i,\ i \in \mathcal{I}\}$, $\mathcal{I} \subseteq \{1, \ldots, n\}$. For piecewise linear functions on triangulated surfaces, the discrete Laplacian operator is defined as $\Delta f(\mathbf{p}_i) = \sum_{j \in N(i)} w_{ij} \left[f(\mathbf{p}_j) - f(\mathbf{p}_i)\right],\ i = 1, \ldots, n$, where $N(i)$ is the set of vertices adjacent to the vertex i and w_{ij} is the weight associated to the directed edge (i, j). As coefficients w_{ij} we can select the *mean-value* [8] or the *cotangent* [20] *weights*, which approximate harmonic maps or minimize the Dirichlet energy respectively. The harmonicity of f is equivalent to the linear system $\mathbf{L}\mathbf{f}^\star = \mathbf{b}$, where $\mathbf{f}^\star := (f(\mathbf{p}_i))_{i \in \{1,\ldots,n\} \setminus \mathcal{I}}$ is the vector of unknowns, $\mathbf{b}$ is a constant vector related to the boundary conditions $\mathcal{B}$, and $\mathbf{L}$ is the *Laplacian matrix*

$$\mathbf{L}(i,j) := \begin{cases} \sum_{k \in N(i)} w_{ik} & \text{if } i = j, \\ -w_{ij} & \text{if } (i,j) \text{ is an edge of } \mathcal{M}, \\ 0 & \text{otherwise.} \end{cases} \tag{1}$$

The eigenvectors $\mathbf{x}_i$ of $\mathbf{L}$ related to the smallest eigenvalues λ_i of (1), $0 = \lambda_0 \leq \lambda_1 \leq \ldots \leq \lambda_{n-1}$, were used in [4] for quadrilateral remeshing; the intrinsic definition and a generally low number of critical points make these functions a natural choice if the harmonicity of f is not strictly required. In this case, the i^{th} scalar field is defined as $f_i := \sqrt{\lambda_i}\mathbf{x}_i$ with $\mathbf{L}\mathbf{x}_i = \lambda_i \mathbf{x}_i, i = 1, \ldots, n-1$; finally, the first eigenvectors are smooth and slowly varying functions, while the last ones show rapid oscillations. If $\mathcal{M}$ is a surface with boundary, we substitute $\mathbf{L}$ with $(\mathbf{L}^T + \mathbf{L})/2$; this choice guarantees that the new Laplacian matrix is symmetric and admits a real eigensystem.

Critical points classification. Given a C^1 function $f : \mathcal{M} \to \mathbb{R}$ defined on a smooth 2-manifold $\mathcal{M}$, the *critical points* of f are defined as those points $\mathbf{p} \in \mathcal{M}$ such that $\nabla f(\mathbf{p}) = \mathbf{0}$ and they correspond to maxima, minima, and saddles of f. In the discrete setting, we adopt the definition provided by Banchoff [2] that classifies a vertex according to the values of f on its neighborhood. More precisely, the vertex $\mathbf{p}_i$ is a *maximum* (resp., *minimum*) if its function value is higher (resp., lower) than those of its neighborhood. Let

$$Lk(i) := \{j_1, \ldots, j_k \in N(i) :\ (j_s, j_{s+1})_{s=1}^{k-1} \text{ edges of } \mathcal{M}\}$$

be the *link* and

$$Lk^{\pm}(i) := \{j_s \in Lk(i) :\ f(\mathbf{p}_{j_{s+1}}) > f(\mathbf{p}_i) > f(\mathbf{p}_{j_s})\},$$

the *mixed link* of i [17], where s is intended as mod $(k+1)$. If the cardinality of $Lk^{\pm}(i)$ is $2 + 2m$, $\mathbf{p}_i$ is classified as a *saddle* of multiplicity $m \geq 1$. Once the vertex-vertex relation has been extracted, the classification procedure requires $O(n)$ time. Figure 2(a) shows the behavior of the iso-contours of a harmonic scalar field f.

If $\mathcal{M}$ has e edges, t faces, and b boundary components, the genus g of $\mathcal{M}$ is given by the relation $g = \frac{1}{2}(2 - \chi(\mathcal{M}) - b)$, where $\chi(\mathcal{M}) := n - e + t$ is the *Euler characteristic*. For a closed surface $\mathcal{M}$, the identity $\chi(\mathcal{M}) = \text{minima} - \text{saddles} + \text{maxima}$ gives the relation between the critical points of $(\mathcal{M}, f)$ and the genus of $\mathcal{M}$ [2, 16].

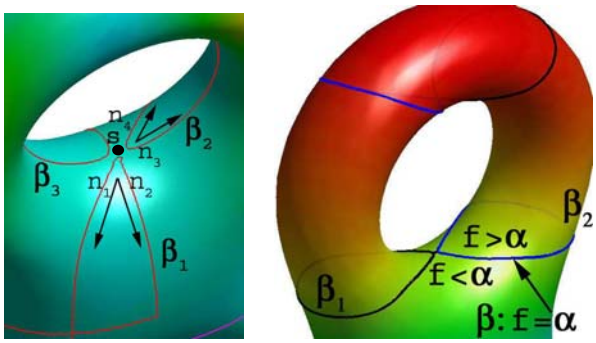

(a) (b)

Figure 3. (a) Iso-contour $\beta := \cup_{i=1}^{3}\beta_i$ of a saddle point $\mathbf{s}$ of multiplicity 2. For the meridian loop β_1 (resp., β_2), the outgoing directions ($\mathbf{n}_1$, $\mathbf{n}_2$) (resp., ($\mathbf{n}_3$, $\mathbf{n}_4$)) are shown. (b) Evaluation of the sign of $f-\alpha$ around $f^{-1}(f(\alpha))$.

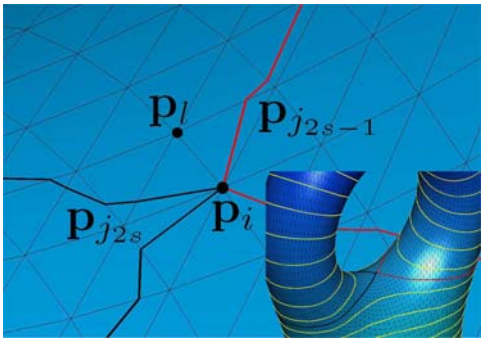

Figure 4. Evaluation of the sign of f at the points of the 1-star of a saddle point $\mathbf{p}_i$.

3 Cut graphs

Under the hypothesis that f is a *Morse* function (i.e., $f \in C^2$ and the Hessian matrix at the critical points is non-singular), this section discusses a novel approach which identifies and cuts the topological handles of $\mathcal{M}$ along the iso-contours of the saddle points of f. This choice does not require to extract the Reeb graph of $\mathcal{M}$ as done in [19, 24, 25], takes $O(n)$ time instead $O(n \log n)$, and identifies a family of cut-graphs and topological generators of $\mathcal{M}$ (see Section 4). To this end, Section 3.1 introduces a procedure to trace the set of iso-contours $\mathcal{S}$ associated to the saddle points of $(\mathcal{M}, f)$, where $\mathcal{M}$ is a $g-$genus triangulated surface with b boundary components. As described in Section 3.2, in $\mathcal{S}$ we identify g loops $\Gamma := \{\gamma_1, \ldots, \gamma_g\}$ such that $\mathcal{M}^\star := \mathcal{M} \setminus (\gamma_1 \cup \ldots \cup \gamma_g)$ is a connected 0-genus surface with $2g + b$ boundary components. Then, in Section 3.3 we review a method which joins these boundary components and converts $\mathcal{M}^\star$ to a disc-like surafce $\overline{\mathcal{M}}$. The degrees of freedom in the choice of Γ and the joining procedure provide a *family* of cut-graphs of $\mathcal{M}$.

3.1 Iso-contours of f at saddle points

Let $f : \mathcal{M} \to \mathbb{R}$ be a Morse scalar field and $\mathbf{p}_i$ a saddle point of multiplicity m such that $f(\mathbf{p}_i) = \alpha$. The connected component β of $f^{-1}(\alpha)$ that contains $\mathbf{p}_i$ (see Figure 3(a)) is the union of $m+1$ closed curves $\beta_1, \ldots, \beta_{m+1}$ that intersect at $\mathbf{p}_i$, that is $\beta := \cup_{s=1}^{m+1}\beta_s \ni \mathbf{p}_i$. For $s = 1, \ldots, m+1$ and $j_{2s-1}, j_{2s} \in Lk^{\pm}(i)$, the vectors $\mathbf{n}_{2s-1} := \mathbf{p}_{j_{2s-1}} - \mathbf{p}_i$ and $\mathbf{n}_{2s} := \mathbf{p}_{j_{2s}} - \mathbf{p}_i$ give the outgoing directions that originate at $\mathbf{p}_i$ and used to trace β_s. These vectors are stored during the classification of the vertices of $\mathcal{M}$ as critical points of f.

Starting from $\mathbf{p}_i$ toward the direction $\mathbf{n}_{2s-1}$, we trace β_s by following the gradient field of f until we come back to $\mathbf{p}_i$ along $\mathbf{n}_{2s}$. Slicing $\mathcal{M}$ along a given *meridian loop* β_s (see Section 3.2) requires to duplicate its points and therefore to know which parts of the triangles intersected by β_s are inside and outside the iso-contour (see Figure 3(b)). Since β_s might have a clockwise or an anti-clockwise orientation, we infer the value of f around β_s by evaluating the sign of $f(\mathbf{p}_l) - \alpha$, where $l \in Lk(i)$ and $\mathbf{p}_l$ is the vertex that we meet walking from $\mathbf{p}_{j_{2s-1}}$ to $\mathbf{p}_{j_{2s}}$ along the 1-star of i (see Figure 4). If l does not exist, the third vertex $\mathbf{p}_j$ of the triangle with edge $\mathbf{p}_i\mathbf{p}_{j_{2s-1}}$ is external to β_s; then, the sign of $f - \alpha$ inside β_s is opposite to that of $f(\mathbf{p}_j) - \alpha$.

If f has s saddles and m_i is the multiplicity of the saddle $\mathbf{s}_i$, we extract at last $s + \sum_{\mathbf{s}_i \text{saddle}} m_i$ meridian loops in linear time. To simplify the discussion, in the following we assume to have simple saddles (i.e., $m = 1$) where f has different values; in this case, we trace $2s$ meridian loops. It follows that the smoothness of f and a low number of saddle points are the properties that should guide the selection of f; for instance, a harmonic scalar field with 1 minimum and 1 maximum has a minimal number of $2g$ saddles, which correspond to $4g$ smooth meridian loops. Other choices are the eigenfunctions of the Laplacian matrix related to the smallest eigenvalues and the scalar field f_{g+1} that provides the embedding of $\mathcal{M}$ on the g^{th} spherical harmonic (see Figure 2(b) at page 3).

3.2 Identifying and cutting the topological handles of $\mathcal{M}$

Let us suppose that we have performed $k < g$ meridian cuts $\{\gamma_1, \ldots, \gamma_k\}$ related to the loops of k saddles of $(\mathcal{M}, f)$; therefore, $\mathcal{M}^\star := \mathcal{M} \setminus \bigcup_{i=1}^{k}\gamma_i$ is a connected surface of genus $g - k$ with $2k + b$ boundary components (see Figure 5(a-b, d-e)). Let $\mathbf{s} \in \mathcal{M}$ be a saddle point that has not yet been visited. To decide if one of the two sub-

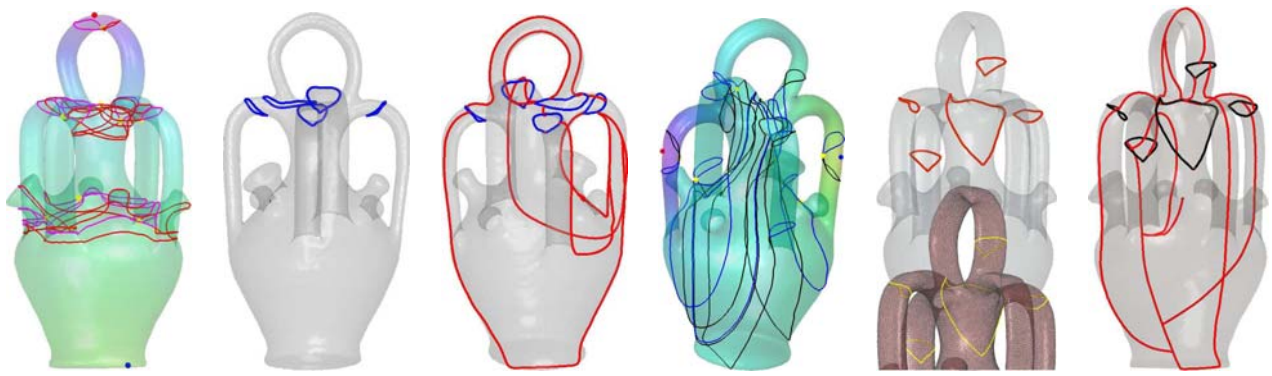

(a) (b) (c) (d) (e) (f)

Figure 5. Pipeline of the cut-graph search: (a) iso-contours related to the saddle points of a harmonic scalar field with 1 maximum, 1 minimum, and 10 saddles; (b) selected meridian cuts; (c) cut-graph with link paths induced by the parameterization domain. (d) Quasi Morse-Smale complex of the first (non-trivial) Laplacian eigenfunction; (e) meridian cuts and (f) cut-graph induced by the distortion metric [19].

loops β_1, β_2 of the connected component of the iso-contour $\beta := f^{-1}(f(\mathbf{s}))$ that contains $\mathbf{p}_i$ is a meridian cut, we calculate the genus $\overline{g}$ and the number of connected components of $\mathcal{M}^\star \setminus \beta_1$ (resp., $\mathcal{M}^\star \setminus \beta_2$). If $\overline{g} = g - (k+1)$ and we did not disconnect $\mathcal{M}^\star$, β_1 (resp., β_2) is marked as possible meridian cut. If both β_1 and β_2 are possible cuts we select the shortest one. Then, we slice $\mathcal{M}^\star$ along the selected meridian cut (if any) and we set it as γ_{k+1}. The algorithm proceeds marking $\mathbf{s}$ as visited and considering the non-visited saddle points until g meridian cuts have been performed (see Figure 5(b, e)). We note that at each step the genus and the number of connected components of $\mathcal{M}^\star$ are evaluated in linear time through the Euler formula and a visit of the faces of $\mathcal{M}^\star$.

Given the scalar field f, the selection of the set $\Gamma := \{\gamma_1, \ldots, \gamma_g\}$ has two degrees of freedom. The first one is the choice of g cuts among $2s$ meridian loops, where s is the number of saddle points of $(\mathcal{M}, f)$. Since the cut-graphs which interpolate points of high-curvature experience a low distortion, we reorder the saddle points in decreasing order of Gaussian (or mean) curvature and we first process those with the highest values. However, other application-driven criteria can be used to select the meridian cuts and reduce the visibility of the seam on the textured/remeshed surface (e.g., minimal length of the meridian cuts, position on the surface). In several cases, such as at the beginning of the iterative procedure where few cuts have been traced, the possibility of selecting the meridian cut between both β_1 and β_2 gives the second degree of flexibility.

3.3 Joining the handle cuts

At this stage, we have a surface $\mathcal{M}^\star$ with $k := 2g + b$ boundary components $\{\gamma_i\}_{i=1}^k$ and 0-genus. Rather than using mesh-traversal techniques to convert $\mathcal{M}^\star$ to a disc-like surface, and in order to overcome their dependence on the mesh connectivity, [19] traces smooth link paths among the boundaries of $\mathcal{M}^\star$ by constructing a bijection $\phi : \mathcal{M}^\star \rightarrow \mathbb{R}^2$ between $\mathcal{M}^\star$ and the parameterization domain. In this case, each link-path between γ_i and γ_j on $\mathcal{M}^\star$ is the counterimage $\phi^{-1}([\mathbf{p}, \mathbf{q}])$ of the line segment $[\mathbf{p}, \mathbf{q}]$ of minimal length which joins $\phi(\gamma_i)$ to $\phi(\gamma_j)$ (see Figure 5(c)). Some variations of this technique enable to join the meridian cuts and the boundary components of $\mathcal{M}$ admitting or discarding bifurcations of the link-paths and to interpolate a source point. A more general strategy [19] defines γ as the minimum of the functional which is a convex combination between the cut length and the related parameterization stretch; this choice avoids having long seams while guaranteeing a low distortion (see Figure 5(f)). Then, as discussed in [10], an iterative procedure can be used to augment the initial cut-graph γ of the disc-like surface $\overline{\mathcal{M}}$ by joining γ to sub-regions of high L^2-stretch until the distortion is below a given threshold. The computational cost is $O(n \log n)$, with n number of input vertices.

4 Homological generators

The degrees of freedom for the selection of the cut-graphs decrease if we search the homology base of $\mathcal{M}$, that is, a pair of a meridian and longitude loop of each topological handle. Homology bases are commonly used for surface

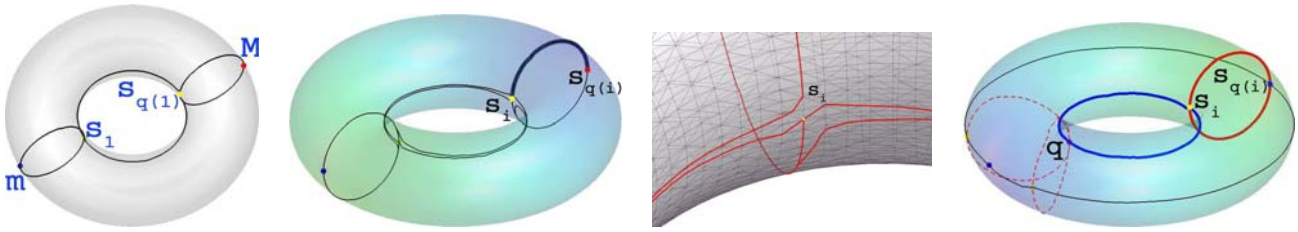

(a) (b) (c) (d)

Figure 6. (a) Topological generators of the torus. Pipeline: (b) quasi Morse-Smale complex of a harmonic function whose flow lines (c) miss the saddle point (yellow circle) and approach a maximum (red point); the marked line shows the shortest path which joins a saddle to a maximum. (d) Construction of a quasi Morse-Smale complex which includes the generators (marked curves) of the handle.

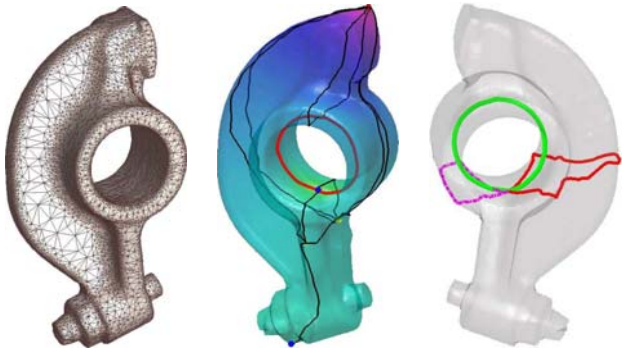

(a) (b) (c)

Figure 7. (a) Input surface; (b) quasi Morse-Smale complex and longitude (red curve) of an irregularly sampled surface. (c) Generators: the meridian is the longest loop (red curve) belonging to the iso-contour of the saddle.

classification and global *conformal* parameterization, i.e. a mapping φ that preserves the angles [11]. As discussed in Section 3, the iso-contours at the saddle points of $(\mathcal{M}, f)$ are used to trace the meridian cuts of the topological handles of $\mathcal{M}$. In this section, we suppose that $\mathcal{M}$ is a closed surface and we evaluate a longitude cut of each handle by combining the quasi Morse-Smale complex of $(\mathcal{M}, f)$ [5] with the construction of harmonic scalar fields introduced in Section 2.

The *descending* (resp., *ascending*) *manifold* of a critical point $\mathbf{p}$ is the set of points of $\mathcal{M}$ that flow towards (resp., originate from) $\mathbf{p}$. The intersection of the ascending and descending manifolds form a complex which is called the *quasi Morse-Smale complex* of f. Moreover, if the two manifolds intersect only transversally, i.e. f satisfies the Morse-Smale condition, then the complex is called *Morse-Smale* and it provides a decomposition of $\mathcal{M}$ into 4-sided cells of uniform behavior of the gradient flow ∇f with two opposite saddles, a maximum and a minimum as corners (see Figure 6(a)). In the discrete case, the quasi Morse-Smale complex can be computed by joining the critical points of f with flow lines of steepest ascent/descent and the Morse-Smale condition is verified *a-posteriori* with respect to the computation of the complex. In our approach, we are interested in extracting the quasi Morse-Smale complex of $(\mathcal{M}, f)$, which is used to guide the computation of the generators of $\mathcal{M}$.

If f is a harmonic scalar field with $2g$ saddles, the ascending flow lines of a saddle point $\mathbf{s}_i$ approaches another saddle $\mathbf{s}_{q(i)}$ and vice versa. Then, we can generate g couples of saddle points $\{\sigma_i := (\mathbf{s}_i, \mathbf{s}_{q(i)})\}_{i=1}^{g}$ and the union of the two flow lines from $\mathbf{s}_i$ to $\mathbf{s}_{q(i)}$ give the longitude cut of the topological handle associated to σ_i (see Figure 6(a)). Even thought it is theoretically possible to choose such a function f [16], a small perturbation of f makes the two ascending flow lines miss the associated saddles and approach a maximum or a minimum without meeting each others (see Figure 6(b-c)). However, having a scalar field with a minimal number of saddle points guarantees that the saddles are located on the topological handles and they are not scattered on $\mathcal{M}$. Therefore, the idea behind our method is to change $\mathbf{s}_i$ into an extremum of an appropriate scalar field on $\mathcal{M}$.

Let us suppose that we change f into a harmonic field $h : \mathcal{M} \rightarrow \mathbb{R}$ with $2g$ saddles in such a way that $\mathbf{s}_i$ becomes an extremum of h. The properties of the quasi Morse-Smale complex $\mathcal{C}$ of $(\mathcal{M}, h)$ guarantee that from a critical point $\mathbf{q}$ of $(\mathcal{M}, h)$ we reach $\mathbf{s}_i$ or a saddle point of h. This fact and the location of $\mathbf{s}_i$ on a topological handle of $\mathcal{M}$ ensure that the flow lines of $\mathcal{C}$ that interpolate $\mathbf{s}_i$ and $\mathbf{q}$ contain a longitude cut (see Figure 6(d)). To build such a function h, we consider all the flow lines of $(\mathcal{M}, f)$ that originate and flow toward the saddle point $\mathbf{s}_i$ and, among them, we select the path of minimal length which joins $\mathbf{s}_i$ to a critical

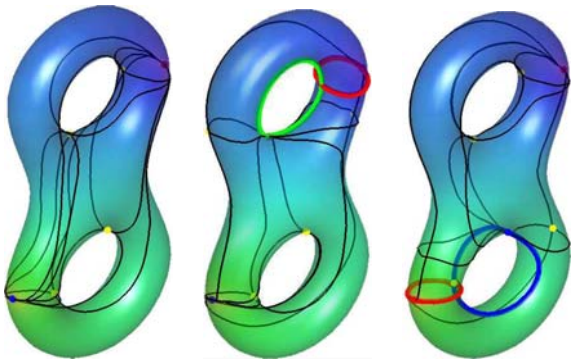

(a) (b) (c)

Figure 8. Quasi Morse-Smale complex of (a) f and (b) of the scalar field h used to extract the generators shown as marked curves. (c) Second iteration.

point $\mathbf{s}_{q(i)}$ (see Figure 6(b)). In the general case, $\mathbf{s}_{q(i)}$ might be a minimum or a maximum and not necessarily a saddle. As next step, we build the harmonic scalar field h with $2g$ saddles and Dirichlet boundary conditions $h(\mathbf{s}_i) = f(\mathbf{s}_{q(i)})$ and $h(\mathbf{s}_{q(i)}) = f(\mathbf{s}_i)$; this choice ensures that $\mathbf{s}_i$ and $\mathbf{s}_{q(i)}$ are the unique extrema of h (see Figure 6(d)). Then, we evaluate the set Θ of loops of the quasi Morse-Smale complex related to $(\mathcal{M}, h)$ that interpolate the saddle $\mathbf{q}$ of h and $\mathbf{s}_i$. Among the loops $\beta \in \Theta$ such that $\mathcal{M} \setminus \beta$ has genus $g-1$, we select the shortest one (see Figure 6(d)).

As done in Section 3.2, we repeat this procedure until g longitudes, which do not disconnect $\mathcal{M}$, have been found. Once the Laplacian matrix $\mathbf{L}$ has been evaluated, at each step h is the solution of a sparse linear system whose coefficient matrix is achieved by removing the rows and columns of $\mathbf{L}$ related to the indices $\{i, q(i)\}$. The computational cost varies from $O(n)$ to $O(n \log n)$, depending on the sparsity percentage of $\mathbf{L}$. The construction of the quasi Morse-Smale complex and the extraction of the generators requires $O(n)$ time.

Chosen a topological handle $\mathcal{H}$ associated to a saddle point $\mathbf{s}_i$ of $(\mathcal{M}, f)$, the procedure generally provides the longitude cut of $\mathcal{H}$ while the meridian cut, which interpolates $\mathbf{s}_{q(i)}$, might be missed; however as discussed in Section 3.1, a meridian cut is always available considering the iso-contour of f at $\mathbf{s}_i$ (see Figure 7). To guarantee that f smoothly varies on $\mathcal{M}$ without regions of constant value, in the examples of the paper we have considered as f a harmonic scalar field whose unique maximum and minimum are (a) those of the first non-trivial Laplacian eigenfunctions with highest curvature values, or (b) the two farthest points of $\mathcal{M}$ (see Figure 8). In Figure 9, a family of topological generators of the bi-torus with a different sampling density is shown.

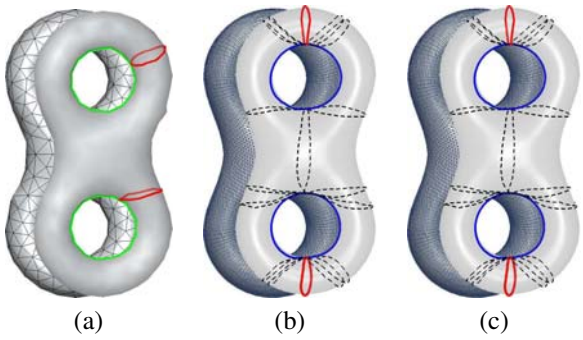

(a) (b) (c)

Figure 9. Longitude together with several meridians of the bi-torus at three levels of details.

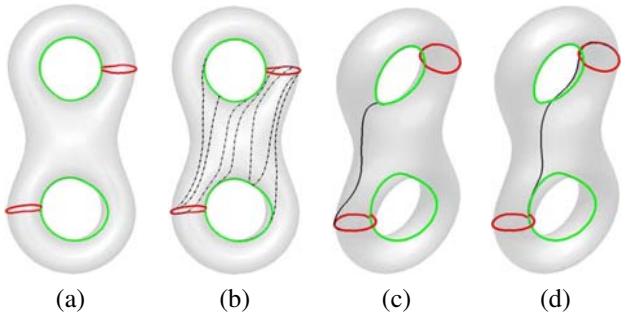

(a) (b) (c) (d)

Figure 10. (a) Generators of the bi-torus; (b) set Γ of flow lines which join the critical points belonging to the generators; (c) shortest path in Γ; (d) shortest path which joins the two saddles used to find the generators.

Joining the handles generators. Once we have identified the meridian γ_i and longitude β_i of each topological handle, we have a new surface $\mathcal{M}^\star$ with $4g$ boundary components which are converted to a cut-graph as described in Section 3.3. Alternatively, since each generator $\sigma_i := \{\gamma_i, \beta_i\}_{i=1}^{g}$ is associated to a saddle point $\mathbf{p}_i$ of $(\mathcal{M}, f)$ the cut-graph is built as the minimum spanning tree of the graph $\mathcal{G}$ induced by the quasi Morse-Smale complex $\mathcal{C}$ of $(\mathcal{M}, f)$. In $\mathcal{G}$, the nodes are the critical points of f, (i, j) is an edge of $\mathcal{G}$ if and only if there exists a flow line of $\mathcal{C}$ from $\mathbf{p}_i$ to $\mathbf{p}_j$ or vice versa, and the weight of (i, j) is the length of the path of minimal length which joins $\mathbf{p}_i$ to $\mathbf{p}_j$ among all the possible ones that can be traced using $\mathcal{C}$ (see Figure 10 and 11(g-h)). This step requires $O(k \log k)$ time, where $k \geq 2g + 2$ is the number of critical points of f. The only caution of using the quasi Morse-Smale complex is to avoid intersections between the handles cuts and the link paths; if they occur, we will use the procedure described in Section 3.3 and that avoids overlapping situations.

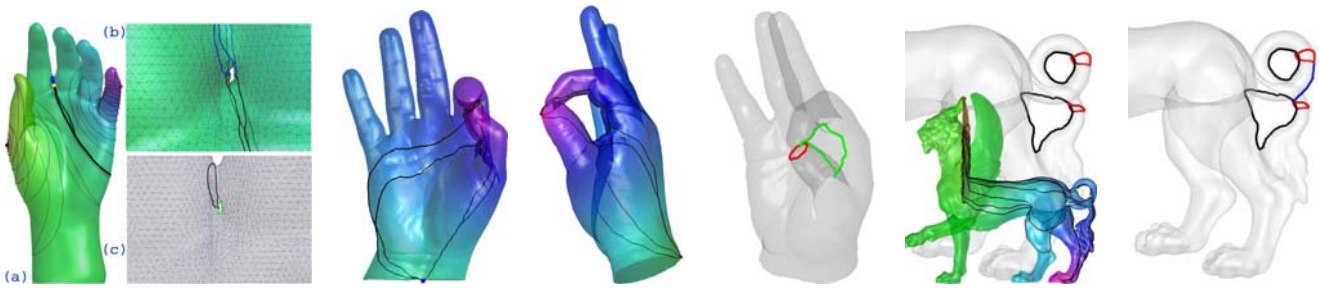

(d) (e) (f) (g) (h)

Figure 11. (a) Quasi Morse-Smale complex, (b) saddle points, iso-contours, and (c) generators of a tiny handle. (d-e) Quasi Morse-Smale complex and (f) topological generators of a 1-genus surface. (g) Quasi Morse-Smale complex, handle generators of a 2-genus surface, and (h) final cut-graph.

Dealing with boundary components. If $\mathcal{M}$ is a surface with boundary, harmonic scalar fields and Laplacian eigenfunctions have several maxima and minima located along the boundary components. This fact does not affect the computation of a family of cut-graphs of $\mathcal{M}$ as described in Section 3, where we consider the iso-contours at saddle points (see Figure 12). The hypothesis that f has 1 maximum and 1 minimum becomes crucial to build a harmonic scalar field with $2g$ saddles and couple them with g longitude cuts. Therefore, the technique described in Section 4 cannot be applied if we have additional extrema due to the boundary components. We can overcome this limitation by closing the boundary components and calculating the handle generators $\mathcal{H}$ as described in Section 4. Since we might have ambiguities in tracing flow lines and building the quasi Morse-Smale complex of $\mathcal{M}$, the cut-graph is constructed from $\mathcal{H}$ as described in Section 3.3 (see Figure 12(d-f)).

5 Numerical analysis of the parameterization with respect to different cut-graphs

In this section, we give an estimation of the "variation" between the parameterizations achieved by using two different cuts γ and β. The idea consists of locating the vertices whose neighborhoods have not been affected by both cuts, and that correspond to a common sub-matrix in the Laplacian matrices of the cut surfaces. Let $\mathcal{M}$ be the input triangulation with $I := \{i : 1 \leq i \leq n\}$ set of vertices, and Laplacian matrix $\mathbf{L}$ related to a given class of weights evaluated using the 1-star of each vertex. Cutting $\mathcal{M}$ along the curve γ (resp., β) converts $\mathcal{M}$ to a new triangulation $\mathcal{M}_\gamma := (M_\gamma, T_\gamma)$ (resp., $\mathcal{M}_\beta := (M_\beta, T_\beta)$) where M_γ has n_γ (resp., n_β) vertices

$$I_\gamma := I \cup \{i : n+1 \leq i \leq n_\gamma\}$$

(resp., $I_\beta := I \cup \{i : n+1 \leq i \leq n_\beta\}$). We now explicit how the Laplcian matrix $\mathbf{L}_\gamma$ (resp., $\mathbf{L}_\beta$) of $\mathcal{M}_\gamma$ (resp., $\mathcal{M}_\beta$) is related to $\mathbf{L}$. Let $N^2(i) := N(N(i))$ be the 2-star of i and

$$J_{\gamma,\beta} := \{i \in I : N^2(i) \cap \gamma = \emptyset \ \wedge \ N^2(i) \cap \beta = \emptyset\}$$

the set of vertices of $\mathcal{M}$ whose 2-stars were not affected by both cuts γ and β. Then, we have that

$$\mathbf{L}_\gamma(i,j) \equiv \mathbf{L}_\beta(i,j) \equiv \mathbf{L}(i,j), \ \forall i \in J_{\gamma,\beta}, \ j \in N(i).$$

With a change of the indices of the vertices in $\mathcal{M}_\gamma$ and $\mathcal{M}_\beta$, we can suppose without loss of generality that $J_{\gamma,\beta} := \{1, \ldots, \overline{n}\}$ and set $\overline{\mathbf{L}} \in \mathbb{R}^{\overline{n} \times \overline{n}}$ as

$$\overline{\mathbf{L}}(i,j) := \begin{cases} \mathbf{L}(i,j) & i \in J_{\gamma,\beta}, \ j \in N(i) \\ 0 & \text{else.} \end{cases}$$

Let $\varphi_\gamma : \mathcal{M}_\gamma \to \mathbb{R}^2$ (resp., $\varphi_\beta : \mathcal{M}_\beta \to \mathbb{R}^2$) be the parameterization of $\mathcal{M}_\gamma$ (resp., $\mathcal{M}_\beta$) with respect to the cut γ (resp., β); these two functions are defined on a common subset $\mathcal{V} := \{\mathbf{p}_i, \ i \in J_{\gamma,\beta}\}$. The parameterization φ_γ (resp., φ_β) is achieved by solving the $n_\gamma \times n_\gamma$ linear system $\mathbf{L}_\gamma \mathbf{x}_\gamma = \mathbf{b}_\gamma$ (resp., $\mathbf{L}_\beta \mathbf{x}_\beta = \mathbf{b}_\beta$ of dimension $n_\beta \times n_\beta$) where

$$\mathbf{L}_\gamma \equiv \begin{bmatrix} \overline{\mathbf{L}} & \mathbf{0} \\ \mathbf{S}_{1,\gamma} & \mathbf{S}_{2,\gamma} \end{bmatrix}, \quad \mathbf{L}_\beta \equiv \begin{bmatrix} \overline{\mathbf{L}} & \mathbf{0} \\ \mathbf{S}_{1,\beta} & \mathbf{S}_{2,\beta} \end{bmatrix},$$

$[\mathbf{S}_{1,\gamma}, \mathbf{S}_{2,\gamma}] \in \mathbb{R}^{(n_\gamma - \overline{n}) \times n}$ (resp., $[\mathbf{S}_{1,\beta}, \mathbf{S}_{2,\beta}] \in \mathbb{R}^{(n_\beta - \overline{n}) \times n}$) is the sub-matrix related to the vertices of $\mathcal{M}_\gamma$ (resp., $\mathcal{M}_\beta$) affected by the cuts and $\overline{\mathbf{L}}$ is a common sub-matrix related to the set of indices $J_{\alpha,\beta}$.

We now estimate the variation of the two parameterizations on $\mathcal{V}$. Let $\overline{\mathbf{x}}_\gamma$ (resp., $\overline{\mathbf{x}}_\beta$), and $\overline{\mathbf{b}}_\gamma$ (resp., $\overline{\mathbf{b}}_\beta$) be the vectors achieved by considering the first $\overline{n}$ components of $\mathbf{x}_\gamma$ (resp., $\mathbf{x}_\beta$) and $\mathbf{b}_\gamma$ (resp., $\mathbf{b}_\beta$); therefore, we have that

$$\begin{cases} \overline{\mathbf{L}}\overline{\mathbf{x}}_\gamma = \overline{\mathbf{b}}_\gamma, \\ \overline{\mathbf{L}}\overline{\mathbf{x}}_\beta = \overline{\mathbf{b}}_\beta. \end{cases}$$

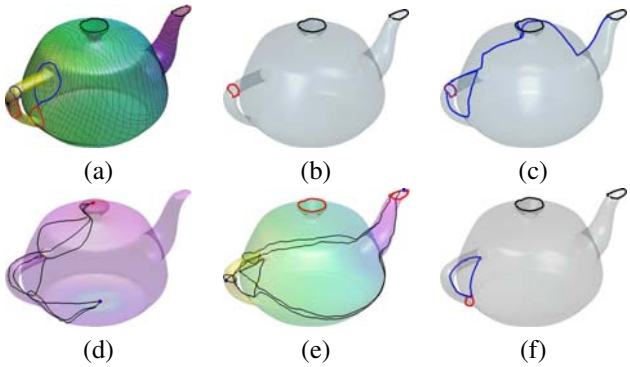

Figure 12. (a) Surface of genus 1 with 2 boundary components and iso-contours at saddle points; (b) meridian cut; (c) cut-gtaph. Quasi Morse-Smale complex of the (d) close and (e) bordered teapot; (f) handle generators.

Table 1. Timings (s:ms) report the evaluation of the cut-graph and the identification of the topological generators. Tests are performed on a Pentium IV 2.80 GHz.

Example	♯Vert.	g	Cut-graph	Top. Gen.
Fig. 1	$60K$	5	34.1	41.2
Fig. 7	$11K$	1	8.3	9.1
Fig. 11(a-b)	$40K$	1	25.4	24.0
Fig. 11(g-h)	$50K$	1	30.4	35.0
Fig. 12(d-f)	$6K$	1	4.5	7.3

It follows that $\|\overline{\mathbf{b}}_\gamma - \overline{\mathbf{b}}_\beta\|_2 \leq \|\mathbf{L}\|_2 \|\overline{\mathbf{x}}_\gamma - \overline{\mathbf{x}}_\beta\|_2$ and

$$\|[\varphi_\gamma(\mathbf{p}_i) - \varphi_\beta(\mathbf{p}_i)]_{i=1,\ldots,\overline{n}}\|_2 \geq \frac{\|\overline{\mathbf{b}}_\gamma - \overline{\mathbf{b}}_\beta\|_2}{\|\overline{\mathbf{L}}\|_2},$$

that is, *the variation between the two parameterizations φ_γ, φ_β on $\mathcal{V}$ has a lower bound which depends on the sub-matrix $\overline{\mathbf{L}}$ related to the part of the triangulation that has not been affected by both cuts, and on the discrepancy of the boundary conditions $\|\overline{\mathbf{b}}_\gamma - \overline{\mathbf{b}}_\beta\|_2$.*

6 Discussion and future work

The paper has presented a method to trace a family of generators and cut-graphs of $\mathcal{M}$ that is simpler and more stable than extracting the Reeb graph and using mesh traversal techniques [19, 24, 25]. In fact, it only requires to evaluate the quasi Morse-Smale complex and the meridian loops at the saddle points of a scalar field f on $\mathcal{M}$.

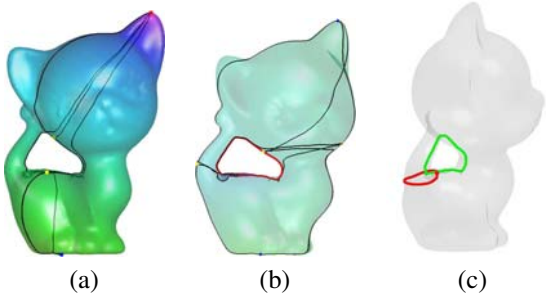

Figure 13. (a) Input quasi Morse-Smale complex; (b) meridian; (c) topological generators.

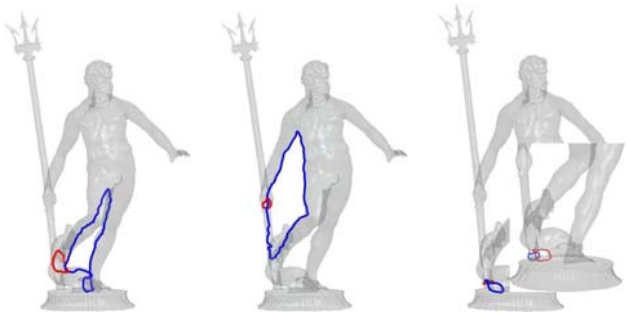

Figure 14. Generators of each topological handle.

In previous work, using mesh traversal techniques for the evaluation of the geodesic metric and the calculation of the minimum spanning tree makes the generators dependent on the mesh tessellation and vertex sampling. This dependence is usually attenuated by a post-process which attempts to make them shorter and smoother. To overcome this drawback, the cut-graphs and topological handles generators have been calculated by tracing the iso-contours and flow-lines of a scalar field f on $\mathcal{M}$. The choice of a smooth scalar field $f : \mathcal{M} \to \mathbb{R}$, which is harmonic or related to the first eigenfunctions of the Laplacian matrix, guarantees to trace smooth meridian loops and flow lines of $(\mathcal{M}, f)$; therefore, the handle generators and the cut-graphs are not noisy and well-shaped. Furthermore, the regularity of f and cutting the surface along paths which do not necessarily interpolate the edges provide smoother results and avoid to apply optimizations steps (e.g., smoothing, search of self-intersections and degenerate cases).

Additional contributions with respect to previous work are: the capability of processing bordered surfaces without assumptions on the regularity of the tessellation and sampling density; a low computational cost which varies from $O(n)$ to $O(n \log n)$; the identification of tiny handles

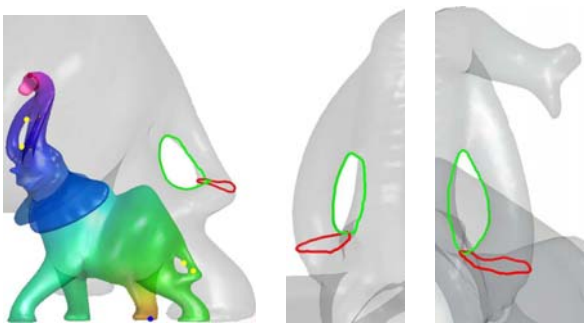

(a) (b) (c)

Figure 15. (a) Input scalar field with 1 maximum, 1 minimum, and 6 saddles; (a-c) generators of each handle.

introduced by the acquisition process (see Figure 11(a-c)). Finally, we provided an estimation of the variation of two parameterizations with respect to different cut-graphs of $\mathcal{M}$. Other examples are given in Figures $13 - 15$ and timings are reported in Table 1. As future work we plan to study the calculation of the topological generators of arbitrary surfaces without using virtual boundary components.

Acknowledgments. This work has been supported by the FP6 IST AIM@SHAPE NoE. Models are courtesy of the AIM@SHAPE Repository, the TSI 3D Models Archive, and the Stanford 3D Scanning Repository.

References

[1] P. Alliez, G. Ucelli, C. Gotsman, and M. Attene. Recent advances in remeshing of surfaces. *Shape Analysis and Structuring, Springer*, 2007.

[2] T. Banchoff. Critical points and curvature for embedded polyhedra. *Journal of Differential Geometry*, 1:245–256, 1967.

[3] E. C. De Verdiere and F. Lazarus. Optimal system of loops on an orientable surface. In *Symposium on Foundations of Computer Science*, pages 627–636, 2002.

[4] S. Dong, P.-T. Bremer, M. Garland, V. Pascucci, and J. C. Hart. Spectral surface quadrangulation. *ACM Transactions on Graphics*, 25(3):1057–1066, 2006.

[5] H. Edelsbrunner, J. Harer, and A. Zomorodian. Hierarchical Morse-Smale complexes for piecewise linear 2-manifolds. *Discrete Comput. Geom.*, 30:87–107, 2003.

[6] J. Erickson and S. Har-Peled. Optimally cutting a surface into a disk. In *ACM Symposium on Computational Geometry*, pages 244–253, 2002.

[7] J. Erickson and K. Whittlesey. Greedy optimal homotopy and homology generators. In *Symposium on Discrete Algorithms*, pages 1038–1046, 2005.

[8] M. S. Floater and K. Hormann. Surface parameterization: a tutorial and survey. In *Advances in Multiresolution for Geometric Modelling*, pages 157–186. 2005.

[9] C. Gotsman, K. Kaligosi, K. Melhorn, D. Michail, and E. Pyrga. Cycle bases of graphs and sampled manifolds. *Computer Aided Geometric Design*, To appear 2006.

[10] X. Gu, S. J. Gortler, and H. Hoppe. Geometry images. In *ACM Transactions on Graphics*, pages 355–361, 2002.

[11] X. Gu and S.-T. Yau. Global conformal surface parameterization. In *Symposium on Geometry Processing*, pages 127–137, 2003.

[12] S. Haker, S. Angenent, A. Tannenbaum, R. Kikinis, G. Sapiro, and M. Halle. Conformal surface parameterization for texture mapping. *IEEE Transactions on Visualization and Computer Graphics*, 6(2):181–189, 2000.

[13] E. Kartasheva. The algorithm for automatic cutting of three-dimensional polyhedrons of h-genus. In *International Conference on Shape Modeling and Applications*, page 26, 1999.

[14] A. Khodakovsky, N. Litke, and P. Schroeder. Globally smooth parameterizations with low distortion. *ACM Transactions on Graphics*, 22(3):350–357, 2003.

[15] H. Lopes, G. Tavares, J. Rossignac, A. Szymczak, and A. Safanova. Edgebreaker: a simple compression for surfaces with handles. In *Symposium on Solid Modeling and Applications*, pages 289–296, 2002.

[16] J. Milnor. *Morse Theory*, volume 51 of *Annals of mathematics studies*. Princeton University Press, 1963.

[17] X. Ni, M. Garland, and J. C. Hart. Fair morse functions for extracting the topological structure of a surface mesh. *ACM Transactions on Graphics*, 23(3):613–622, 2004.

[18] G. Patanè, M. Spagnuolo, and B. Falcidieno. Para-graph: graph-based parameterization of triangle meshes with arbitrary genus. *Computer Graphics Forum*, 23(4):783–797, 2004.

[19] G. Patanè, M. Spagnuolo, and B. Falcidieno. Families of cut-graphs for bordered meshes with arbitrary genus. *Graphical Models*, To appear, 2007.

[20] U. Pinkall and K. Polthier. Computing discrete minimal surfaces and their conjugates. *Experimental Mathematics*, pages 15–36, 1993.

[21] P. V. Sander, Z. J. Wood, S. J. Gortler, J. Snyder, and H. Hoppe. Multi-chart geometry images. In *Symposium on Geometry Processing*, pages 146–155, 2003.

[22] A. Sheffer and J. C. Hart. Seamster: inconspicuous low-distortion texture seam layout. In *Visualization '02*, pages 291–298, 2002.

[23] A. Sheffer, B. Levy, M. Mogilnitsky, and A. Bogomyakov. Abf++: fast and robust angle based flattening. *ACM Transactions on Graphics*, 24(2):311–330, 2005.

[24] D. Steiner and A. Fischer. Cutting 3D freeform objects with genus-n into single boundary surfaces using topological graphs. In *Symposium on Solid Modeling and Applications*, pages 336–343, 2002.

[25] D. Steiner and A. Fischer. Growing surface methods for cutting 3d freeform objects with genus-n. In *Bi-National UK-Israel Conference on "Geometric Modeling Methods"*, 2002.

[26] R. Zayer, C. Rössl, and H.-P. Seidel. Setting the boundary free: A composite approach to surface parameterization. In *Symposium on Geometry Processing*, pages 91–100, 2005.